Available online at www.sciencedirect.com

ScienceDirect

journal homepage: www.elsevier.com/locate/he

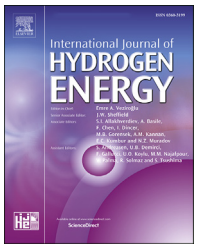

Metal hydride hydrogen storage tank for fuel cell utility vehicles

Mykhaylo Lototskyy [a,*], *Ivan Tolj* [b], *Yevgeniy Klochko* [a], *Moegamat Wafeeq Davids* [a], *Dana Swanepoel* [c], *Vladimir Linkov* [a]

[a] *HySA Systems Competence Centre, South African Institute for Advanced Materials Chemistry (SAIAMC), University of the Western Cape, Bellville 7535, South Africa*

[b] *University of Split, Faculty of Mechanical Engineering and Naval Architecture, Department of Thermodynamics and Heat Engines, Split 21000, Croatia*

[c] *TF DESIGN (Pty) Ltd., Stellenbosch 7600, South Africa*

ARTICLE INFO

Article history:
Received 23 January 2019
Received in revised form
3 April 2019
Accepted 12 April 2019
Available online 4 May 2019

Keywords:
Hydrogen storage
Metal hydrides
Fuel cell utility vehicles

ABSTRACT

The "low-temperature" intermetallic hydrides with hydrogen storage capacities below 2 wt % can provide compact H_2 storage simultaneously serving as a ballast. Thus, their low weight capacity, which is usually considered as a major disadvantage to their use in vehicular H_2 storage applications, is an advantage for the heavy duty utility vehicles. Here, we present new engineering solutions of a MH hydrogen storage tank for fuel cell utility vehicles which combines compactness, adjustable high weight, as well as good dynamics of hydrogen charge/discharge. The tank is an assembly of several MH cassettes each comprising several MH containers made of stainless steel tube with embedded (pressed-in) perforated copper fins and filled with a powder of a composite MH material which contains AB_2- and AB_5-type hydride forming alloys and expanded natural graphite. The assembly of the MH containers staggered together with heating/cooling tubes in the cassette is encased in molten lead followed by the solidification of the latter. The tank can provide >2 h long H_2 supply to the fuel cell stack operated at 11 kWe (H_2 flow rate of 120 NL/min). The refuelling time of the MH tank (T = 15–20 °C, $P(H_2)$ = 100–150 bar) is about 15–20 min.

Introduction

Compact, low energy consuming and safe hydrogen storage is vital to successful implementation of efficient and environment friendly hydrogen and fuel cell technologies in a number of stationary, portable and mobile applications. Various methods of hydrogen densification via compression, liquefaction or interaction with liquid- or solid-state hydrogen storage materials are in focus of international R&D activities for the advancement of hydrogen and fuel cell power systems [1–6].

Metal hydrides (MH) formed by a reversible reaction of gaseous H_2 with a parent hydride forming metal, alloy or intermetallic compound are promising solid-state hydrogen storage materials for various end-user applications. The use of MH allows to achieve a very high volumetric hydrogen storage density, exceeding 100 gH/L in a unit volume of solid-state storage material [3,6,7]. Modest H_2 equilibrium pressures at

* *Corresponding author.*
E-mail address: mlototskyy@uwc.ac.za (M. Lototskyy).

https://doi.org/10.1016/j.ijhydene.2019.04.124
0360-3199/

ambient temperatures in combination with endothermic nature of the MH decomposition result in high intrinsic safety of MH-based hydrogen storage systems. Finally, the ability of extremely broad variation of thermodynamic characteristics of the hydrogen – metal systems by the variation of the composition of the parent material allows to achieve exceptional flexibility of the MH based systems which can be used for hydrogen storage and its controlled supply at pressure/temperature conditions suitable for the customer needs [6–8]. Due to unique combination of their properties, MH, in addition to hydrogen storage, are also used in a number of related applications including thermally driven H_2 compression, thermal management, etc. [8].

The use of fuel cells (FC) in heavy duty utility vehicles, including material handling units/forklifts, has a number of advantages over similar battery-driven vehicles including: (i) constant power during the entire shift, and (ii) shorter refuelling time as compared to the time required to recharge the battery [7,9,10].

Most of the fuel cell power systems for forklifts demonstrated so far have utilised compressed hydrogen stored in gas cylinders (CGH2) at pressures up to 350 bar [11]. However, in comparison to lead-acid batteries, which are conventionally used in the electric forklifts, all commercially available forklift fuel cell power systems with CGH2 hydrogen storage tanks [12–14] are too light and require additional ballast for a proper counterbalancing to provide vehicle stability when lifting rated loads.

The application of MH for hydrogen storage in the fuel cell powered forklifts [8,10,15] and similar utility vehicles (e.g., underground mining vehicles [16]) is a promising option. The "low-temperature" intermetallic hydrides with hydrogen storage capacities below 2 wt% (i.e. storage of 1 kg H requires more than 50 kg of the MH material) can provide compact H_2 storage simultaneously serving as a ballast. Thus, the low weight capacity of intermetallic hydrides, which is usually considered as a major disadvantage to their use in vehicular hydrogen storage applications [1,2], is an advantage for the heavy duty utility vehicles [7,10]. The use of metal hydrides for the storage of hydrogen fuel, where the MH additionally serves as a ballast/counterweight, was described in a number of patents [17–20]. General features of these solutions include placement of a metal hydride hydrogen storage material in a plurality of metal hydride containers which supply hydrogen fuel to a hydrogen engine or fuel cell and are equipped with a means for their heating to provide H_2 desorption from the metal hydride by transferring the heat released during the engine or fuel cell operation to the MH containers.

A metal hydride hydrogen storage tank for forklift applications was developed by Hawaii Hydrogen Carriers LLC, together with other companies and institutions [21]. The tank is made as a staggered array of tubular containers filled with an AB_5-type MH material and placed in a water tank. The hydride tank has dimensions 470 mm (L) x 700 mm (W) x 370 mm (H), contains about 2 kg (~20 Nm^3) H_2 and has an estimated weight about 500 kg when filled with water. The tank, together with other components of the fuel cell power module, was integrated in Crown electric forklift with lifting capacity of 5000 lb (~2.3 tonnes). To provide sufficient counterweight, all the components were assembled within rectangular metal casting body, and the most of its internal volume was occupied by the MH tank.

As it can be seen from the example presented above, main challenge of a conventional solution (MH containers in a water tank) is still insufficient system weight/too big size of the H_2 storage system leaving too small space for the placement of the fuel cell and its Balance of Plant (BoP). The cramped placement of the latter, in turn, creates problems in the access to the components during their assembling and service. As a rule, for even minor service or repair works, the heavy (~2 tonnes) fuel cell power module must be taken away from a vehicle and partially disassembled.

In this work, we present engineering solutions [22,23] of a MH hydrogen storage tank for FC utility vehicles which combines compactness, adjustable high weight, as well as good dynamics of hydrogen charge and discharge.

Layout features and performance

Metal hydride material

Fig. 1 shows pressure–composition isotherms of a C14-AB_2 Laves-type alloy ($A = Ti_{0.55}Zr_{0.45}$; B=Fe + Cr + Mn + Ni) used in this application, as well as in the earlier developments of MH hydrogen storage units at HySA Systems [24,25]. At the room temperature the alloy has an equilibrium H_2 absorption pressure below 10 bar, but due to the necessity to provide a reasonably short refuelling time during H_2 charge, the applied pressure should be higher. The material has a very low absolute value of hydrogenation enthalpy ($\Delta H = -18.5$ kJ/mol H_2; $\Delta S = -78.1$ J/(mol H_2 K)) thus minimizing the heat release during the refuelling and heat absorption during H_2 supply to the FC stack. The alloy exhibits reversible H_2 storage capacity at the typical operating conditions about 170 NL H_2/kg (see Fig. 1).

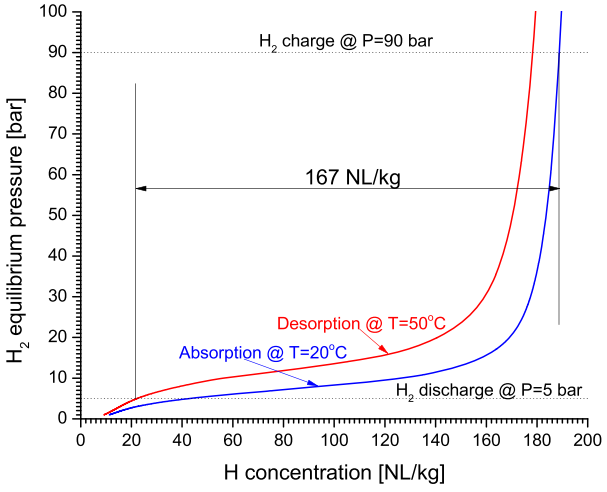

Fig. 1 – Hydrogen absorption and desorption isotherms for the AB_2-type hydrogen storage alloy used in the MH tank. The isotherms were plotted on the basis of the experimental data further processed by a model [26].

The AB_2-type alloy loaded in the tank as a non-activated coarse powder (particle size up to 1 mm) additionally contained 10 wt % of $La_{0.8}Ce_{0.2}Ni_5$ to facilitate its activation.

Metal hydride container

In this development, we upgraded a basic design of the MH container previously developed for the MH hydrogen storage extension tank for commercial forklift fuel cell power module [9]. The container was made of a standard SA 312 sch 40 TP316 1.5 inch seamless tube (OD = 48.26 mm, WT = 3.68 mm, L = 738 mm) welded to forged SS 316 end caps. The front end cap additionally comprised an ¼'' OD SS 316 pipeline for H_2 input/output, with a short tubular sintered stainless steel filter (0.5 μ grade) welded to its end and plugged by welding from the other side. The end with the filter was inserted into the MH container (depth about 60 mm) using a bored-through compression fitting attached to the front end cap by welding. In doing so, the container was made as all-welded stainless steel structure rated for H_2 pressures up to 185 bar at temperatures up to 150 °C and allowing a short-term heating to ≤500 °C when not pressurised.

For the improvement of heat transfer inside the MH bed, the container was equipped with internal perforated copper fins firmly pressed into the tube at 5 mm spacing. The MH powder additionally contained 1 wt % of expanded natural graphite (ENG) for further improvement of heat transfer in combination with protection of walls of the containment against stresses which appeared due to swelling of the MH particles in the course of hydrogenation and were absorbed by the ENG additive. As distinct from conventionally used solutions which provide pre-compacting of the MH − ENG composites before their loading in the container as pellets [27,28], in our case the formation of "compacted" MH bed was achieved by the forces generated during the first hydrogenation due to volume increase of the parent MH material, after optimisation of characteristic inner dimensions of the MH container, ENG content and MH filling density [22].

The powder (~3 kg) was loaded in the container (void volume about 0.94 L) before the welding of the front end cap. The facilitation of mass transfer along the MH bed was provided by an auxiliary tubular gas filter plugged from both ends and installed on the axis of the internal space of the container.

According to South African safety regulations [29], the developed MH containers fall into SEP (sound engineering practice) category. At the same time, the following safety measures have been undertaken during its in-house design and post-manufacturing tests:

- design according to ASME 8 Div 1;
- X-ray tests of all weld joints performed on each container (40 pieces in total);
- pressure test of each container with N_2 (P = 240 bar) witnessed by an approved inspection authority.

According to further test results, the MH containers had hydrogen storage capacity about 0.5 Nm^3 H_2 each; the charge time of the container cooled in a circulated water bath (T = 20 °C) was below 10 min at H_2 supply pressure of 60 bar. Further optimisation of the AB_2-type MH material, by introducing V and reduction of Fe content balanced with Mn from the B-side, as well as increase of Ti:Zr ratio from the A-side to 0.85:0.15 [25] allowed us to increase the H_2 storage capacity by 24% at the same conditions. The optimised material will be used for similar applications on the later stage because its development was completed already after the series of 40 MH containers for the hydrogen storage tank described in this work and loaded with the non-optimised AB_2 alloy (Ti:Zr = 0.55:0.45, no V) has been manufactured.

MH cassette

According to our solution [23], the hydrogen storage tank for utility vehicle applications comprises of several MH cassettes formed by an assembly of the MH containers staggered together with heating/cooling tubes encased in a molten metal or alloy (further solidified). Importantly, the metal or alloy (e.g. lead) should combine high density with melting/solidification point below the maximum allowed operation temperature of the metal hydride container but above the activation temperature of the loaded metal hydride material.

A schematic layout of the MH cassette is presented in Fig. 2, top.

The cassette (*10*) comprises of five MH containers (*11*; see previous section in more details) connected to gas manifold (*12*) which is ended by an external pipeline (*13*; SS 316, ¼'' OD). Heating/cooling accessories (*14*) are made of pieces of ½'' OD stainless steel tubing placed in between the containers *11*, connected in sequence and ended by pipelines (*15*, *16*) for the input and output of a heating/cooling fluid (water or water–glycol mixture). The components are located within a filling body (*17*) formed by the solidification of molten lead.

Fig. 2, bottom, shows image of the pre-assembled MH cassette before lead encasing. The components *11* and *14* of the cassette (the numbering corresponds to Fig. 2, top) are placed in a removable pre-assembly case (*18*)[1] opened from the top and made of stainless steel sheets; all the gaps in the case *18* were closed with a heat-resistant sealant.

Fig. 3 illustrates the procedure of the lead encasing carried out at a specialised foundry. The empty space of the case (*18* in Fig. 2, bottom) was filled by a pre-melted lead followed by the solidification and cooling. Importantly, during the lead encasing, the inner space of the MH containers has to be permanently evacuated via a shut-off valve (*19* in Fig. 2, bottom) installed at the end of the gas pipeline (*13* in Fig. 2). After cooling the cassette down, the evacuation was followed by introducing a pressurised argon, to protect the MH material activated during the lead encasing against oxidation with ambient air (e.g., after accidental opening of the valve *19* disconnected from the evacuation line) that can result in the loss of hydrogen sorption properties of the material.

Typical sequence of the operations during lead encasing (Fig. 3) is described below:

[1] We note that target weight of the cassette (~150 kg in our case) can be adjusted at the design stage by a variation of the length of the filling body (*17*) determined by the length of case (*18*) which can cover main components of the cassette (*11*, *12*, *14*) either completely or partially.

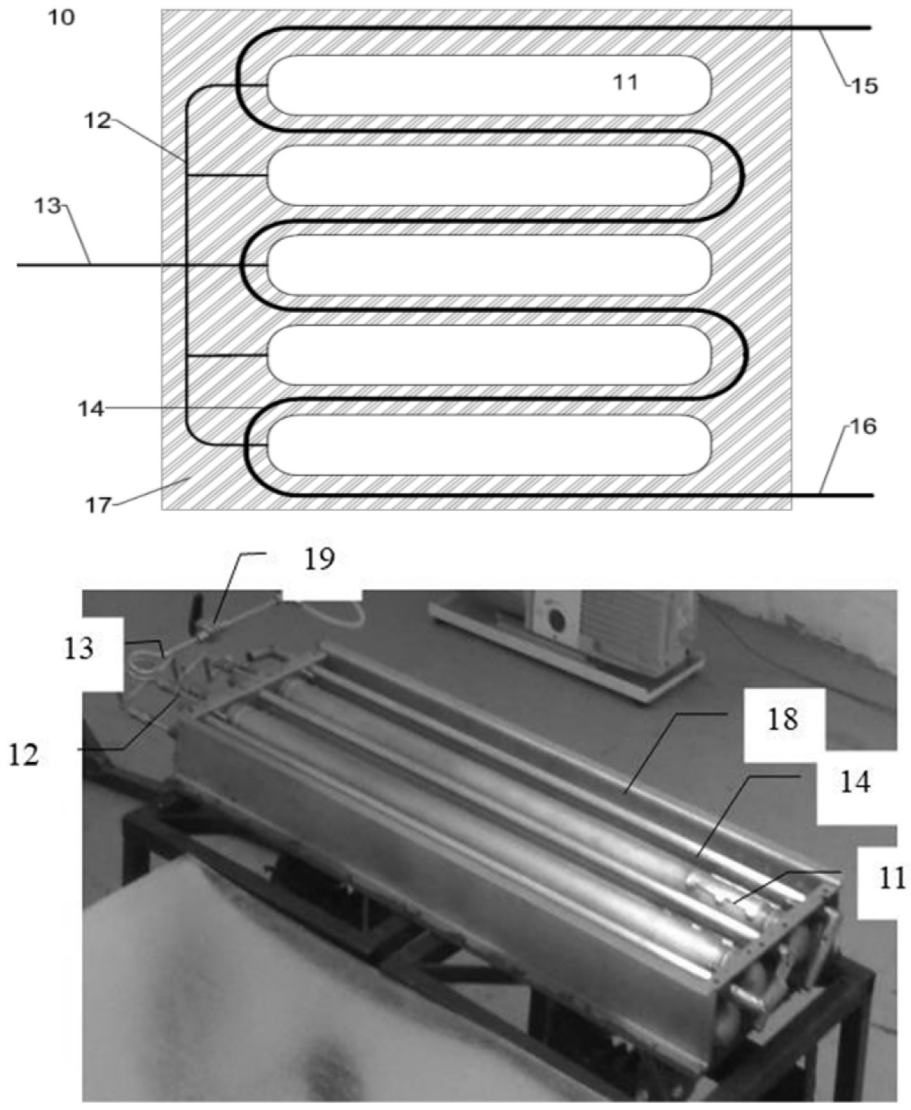

Fig. 2 – Top: schematic layout of the MH cassette [23], bottom: pre-assembled MH cassette before lead encasing.

a. Pre-evacuation of a cold pre-assembly to 10^{-2} mbar.
b. Pre-heat of the assembly up to ~170 °C (the temperature was measured by a K-type thermocouple built into cassette, also assisted by optical pyrometer) during 20 min.
c. Casting of the pre-melted lead (T~350 °C) into pre-assembly case (*18* in Fig. 2, bottom) during 10 min. When carrying out stages b and c, the pressure in the evacuated system increased to 2 mbar (due to desorption of gas and vapour

Fig. 3 – Lead encasing.

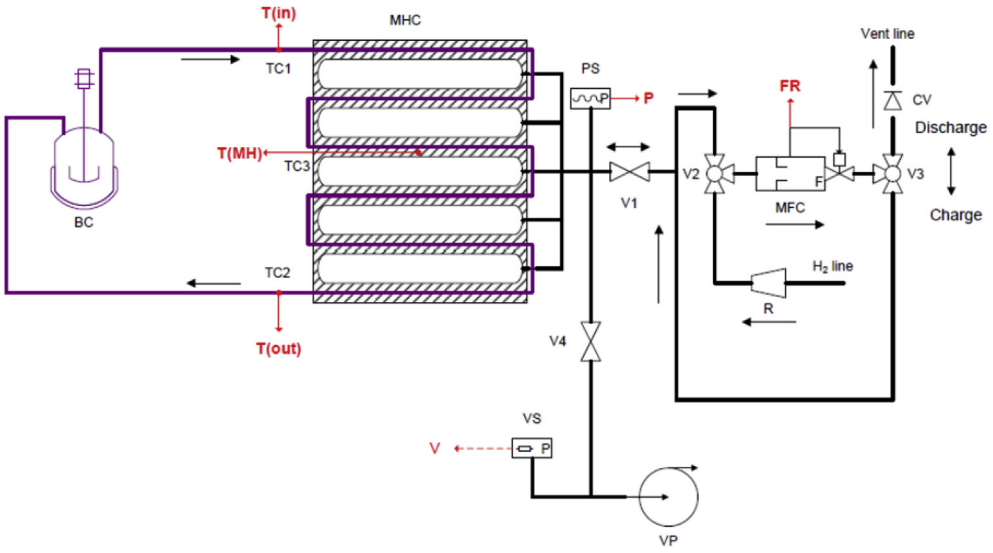

Fig. 4 – Schematic diagram of the setup for final activation and testing of the MH cassette.

species adsorbed on the inner surface of the MH containers, as well as on the particles of the MH load) followed by a gradual decrease to 0.1 mbar before the end of the lead casting.

d. Continuing the evacuation during the cooling of the cassette filled with lead down to T~90 °C. The vacuum at this point was better than $5 \cdot 10^{-2}$ mbar.
e. Filling the cassette with pressurised (~50 bar) argon.
f. After cooling the lead encased and argon-filled cassette to the room temperature and its moving from the lead encasing foundry to HySA Systems, the case (*18* in Fig. 2, bottom) was removed, and the cassette (960 × 269 × 88 mm; weight 144 kg) was connected to a setup for performing the final activation procedure.[2] Further details will be presented below.

Fig. 4 shows piping diagram of the setup for final activation and testing of the MH cassettes. The gas pipeline of the cassette is connected to a gas manifold of the setup equipped with a pressure sensor (*PS*; 0–250 bar) and connected, via shut-off valves *V1* and *V4* to H_2 charge/discharge and evacuation systems, respectively. The H_2 charge/discharge system includes mass flow controller (*MFC*; 0–50 NL H_2/min) and two remotely controlled 3-way valves (*V2* and *V3*). Depending on the positions of the valves *V2* and *V3*, an operator can switch between *Charge* and *Discharge* modes; in both cases a unidirectional hydrogen flow via mass flow controller (*MFC*) is provided. In the *Charge* mode, hydrogen is supplied to the cassette (*MHC*) from *H_2 line*, via reducer (*R*). In the *Discharge* mode, hydrogen is released from the cassette (*MHC*) to *Vent line*, via check valve (*CV*). The evacuation system comprises of a rotary vacuum pump (*VP*) and a Pirani vacuum sensor (*VS*).

The MH cassette is heated and cooled by a water bath circulator (*BC*; controlled circulation flow rate in the range 3–7 L/min) connected to the input and output pipelines (*15*, *16* in Fig. 2, top). The connections of the water pipelines to the cassette are equipped with K-type thermocouples for the measurement of water temperature at the input (*TC1*) and output (*TC2*) of the cassette, respectively. One more K-type thermocouple (*TC3*) was built in the cassette by attaching, before lead encasing, to the wall of one of MH containers in the middle.

The parameters logged during the tests included H_2 pressure (*P*) at the entrance to the gas manifold, H_2 charge/discharge flow rate (*FR*), water temperatures at the input (*T(in)*) and output (*T(out)*) of the cassette, as well as the temperature of MH container in the cassette (*T(MH)*). Also, vacuum (*V*) was monitored during the evacuation.

The final activation of the cassette included release of argon followed by evacuation to $3 \cdot 10^{-2}$ mbar and introducing H_2 at line pressure of 50 bar; all the operations were carried out at the room temperature, without circulation of the heating/cooling water. Hydrogen absorption in the MH started immediately testified by maximum H_2 flow (*FR*), 40 NL/min, equal to the upper limit set by mass flow controller (*MFC*), and gradual increase of the temperature (*T(MH)*). The maximum H_2 flow of 40 NL/min remained unchanged during 40 min followed by a decrease at *T(MH)* > 60 °C (grown from starting 25 °C). After the cooling of the tank was switched on (*T(in)* ~20 °C), the maximum flow of the absorbed H_2 restored immediately and remained constant during 10 min followed by a gradual decrease. The total (integrated) amount of H_2 absorbed in the cassette during 100 min of the first H_2 charge (when the H_2 flow rate decreased below 4 NL/min) was of 2.59 Nm^3, close to the calculated value of 2.5 Nm^3. Similar values of the total H_2 amount absorbed in/desorbed from the MH cassette (2.5–2.7 Nm^3) were observed in the course of the next H_2 charge/discharge cycles.

Typical H_2 charge performance of the MH cassette during the following discharge – charge operation cycles is shown in Fig. 5, left. It is seen that at *T(in)* = 20 °C and water flow about

[2] The time from the end of the lead encasing and the start of the final activation of the cassettes varied from 1 day to 1 week.

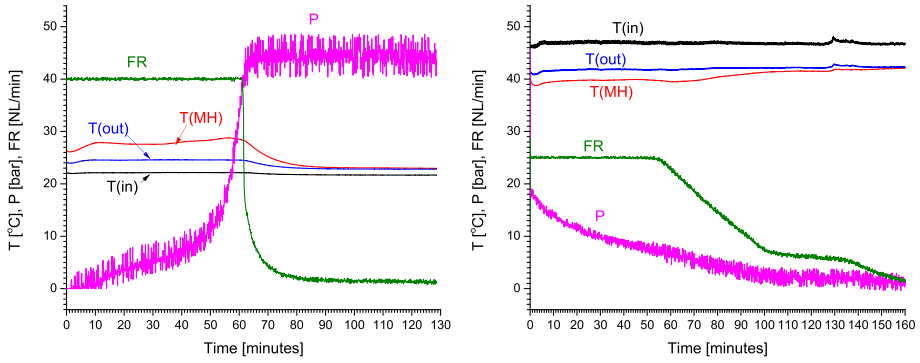

Fig. 5 – H_2 charge (left; water flow at $T = T\,(in)$ 5.2 ± 0.1 L/min) and discharge (right; water flow at $T = T\,(in)$ 6.9 ± 0.1 L/min) performance of the MH cassette.

5 L/min, the maximum H_2 flow rate of 40 NL/min[3] can be maintained during ~1 h. In doing so, the H_2 pressure (P) slowly increases from zero to ~10 bar in first 50 min followed by a fast increase up to the line pressure (40–45 bar) during the next 10–15 min. Such behaviour can be explained by an equilibration between the pressure of H_2 gas and H concentration in the MH material when time dependence of the pressure approximately follows the pressure – composition isotherm (sloping plateau at $P = 3$–10 bar/$T = 20$ °C; see Fig. 1).

The temperature differences ($T(MH)$–$T(in)$) and ($T(out)$–$T(in)$) during H_2 absorption at a constant H_2 flow rate were about 8 and 5 °C, respectively, followed by a gradual decrease when the H_2 flow rate decreased.

Fig. 5, right presents typical H_2 discharge performance of the MH cassette. A summary of the performances measured at different temperatures and flow rates of the heating water is presented in Fig. 6 and Table 1. In all the experiments, the maximum limit of H_2 flow rate set by the flow controller was 25 NL/min, or ~20% higher than a nominal H_2 flow rate (20.83 NL/min) per one cassette of eight in the hydrogen storage tank (see Section MH hydrogen storage tank and its integration in fuel cell power module) required to provide the operation of fuel cell stack at a maximum electric power (15 kW).

During H_2 discharge (Fig. 5, right), the H_2 pressure quickly drops to ~20 bar followed by a gradual decrease. The maximum H_2 flow rate is maintained during 40–60 min followed by almost linear decrease of the flow rate. In doing so, the temperature differences ($T(in) - T(MH)$) and ($T(in) - T(out)$) during H_2 desorption at a constant flow rate were about 6 and 3–4 °C, respectively; the MH temperature then gradually increases approaching the value of $T(out)$ which remains almost the same.

As it can be seen from Fig. 6 and Table 1, the main factor affecting the H_2 discharge performance is the heating temperature whose decrease below 40 °C results in a significant decrease of H_2 amount desorbed at a specific discharge flow rate. This effect becomes more pronounced when the discharge flow rate increases, particularly, when exceeding 10 NL/min, or ~50% of the H_2 flow rate necessary for the operation of the fuel cell stack at full capacity. At $T(in) > 45$ °C, the discharge performance of the MH cassette remains almost the same when the decrease of the H_2 flow rate from 25 to 5 NL/min

[3] Introducing the upper limit of the H_2 flow rate, both in the charge and the discharge modes, was necessary to provide measurements of H_2 flow within the range of the used mass flow controller and, accordingly, proper calculation of the total amount of H_2 absorbed in or desorbed from the cassette.

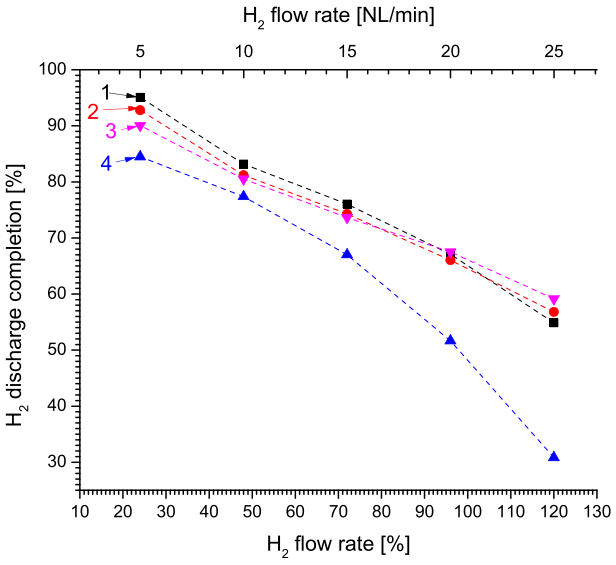

Fig. 6 – Dependence of discharge completion in % of the full H_2 storage capacity (2.5 Nm^3) of the MH tank on the H_2 output flow rate (100% = 20.83 NL/min). Experimental conditions of series 1–4 are specified in Table 1.

Table 1 – H_2 desorption conditions. Accuracies of the control of the process parameters are ±1 °C and ±0.1 L/min, for water input temperature and flow rate, respectively.

Series number (Fig. 6)	$T(in)$ [°C]	Water flow rate [L/min]
1	46	3.0
2	47	6.9
3	55	6.9
4	38	6.9

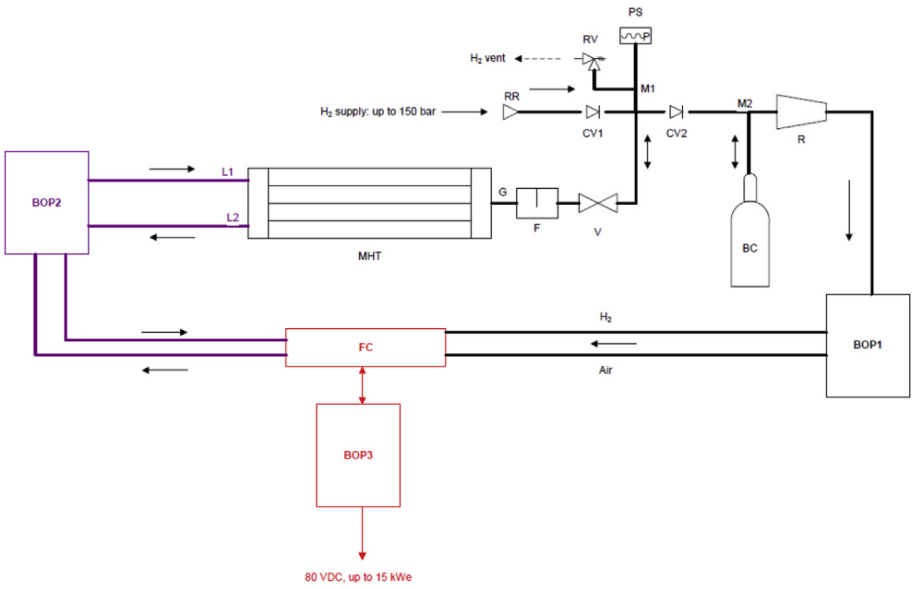

Fig. 7 – *Simplified schematic diagram of the integration of the MH tank in forklift power module.*

results in the increase of the amount of desorbed hydrogen from 55–60% to >90% of the full hydrogen storage capacity.

MH hydrogen storage tank and its integration in fuel cell power module

The MH tank comprising of eight lead-encased MH cassettes described above was integrated in a power module for STILL RX60-30 L electric forklift. The power module jointly developed by HySA Systems and Hot Platinum (Pty) Ltd (South Africa) provides output electric power up to 15 kW in average (up to 30 kW peak power) at bus voltage of 80 VDC and has dimensions 840 (L) x 1010 (W) x 777 (H) mm and weight between 1800 and 1900 kg that corresponds to the admissible weight of the forklift lead acid battery. The power module (see schematic diagram in Fig. 7 and general views in Fig. 8) includes liquid cooled Ballard 9SSL fuel cell stack (*FC*) whose operation is provided by three BoP systems: system for controlled supply of the fuel (H_2) and the oxidant (air) (*BOP1*); stack cooling system (*BOP2*); and power conditioning and control system (*BOP3*). The H_2 fuel consumption of the power module operating at the maximum power of 15 kW was estimated as 166.65 NL/min that corresponds to the value of 20.83 NL/min per one cassette as it was specified in the previous section.

The MH tank (*MHT*) is located in the bottom part of the power module and occupies about ¼ of its inner space (see Fig. 8).

Both gas and heating/cooling liquid pipelines of the eight cassettes are connected in parallel. The common gas pipeline, via auxiliary components, is connected to hydrogen supply port of the gas supply system (*BOP1*) while the common heating/cooling pipelines are connected to the cooling system (*BOP2*) of the fuel cell stack.

As shown in Fig. 7, the gas pipeline (*G*) of the tank (*MHT*), is connected, via an additional 0.5 μ grade inline filter (*F*) and a shut-off valve (*V*) to a gas manifold (*M1*) connected to a pressure sensor (*PS*; 0–250 bar) and safety relief valve (*RV*; set cracking pressure 180 bar) which releases gas to *H_2 vent* pipeline in a case of overpressure. The gas manifold *M1*, via check valve *CV1*, is connected to a refuelling receptacle (*RR*) and, via check valve *CV2*, to a second gas manifold (*M2*) connected to a buffer cylinder (*BC*; 9 L in the volume) and pressure reducer (*R*) to supply H_2 to the gas supply system of the fuel cell BoP (*BOP1*) at the pressure of 0.3–0.5 bar gage.

The heating/cooling pipelines (*L1, L2*) of the tank integrated with the cooling system of the fuel cell stack (*BOP2*) provide heating of the MH cassettes when the stack is operating, or their cooling during H_2 refuelling, by a flow of water/glycol mixture heated by the stack in the operation mode and cooled by a radiator – fan assembly (*RF* in Fig. 8) in the refuelling mode.

Introducing of the buffer cylinder allows to realise a concept of "distributed hybrid" hydrogen storage and supply system which significantly improves performance of H_2 supply from the MH to the fuel cell stack when its power and, in turn, H_2 consumption fluctuate in wide limits [30]. Additionally, presence of check valve (*CV2* in Fig. 7) between the MH tank and the buffer eliminates problem of the system start-up when H_2 pressure in the MH gas manifold (*M1* in Fig. 7) after the end of operation (H_2 desorption at *T*~50 °C) and subsequent cooling down to ambient temperature (e.g. <20 °C) accompanied by H_2 absorption in the MH material can drop below the lower limit of H_2 pressure (~0.3 bar gage) necessary for the normal system operation.

Results of preliminary tests of the MH tank integrated in the fuel cell forklift power module showed that the tank can supply H_2 to the fuel cell stack at H_2 flow rate of 120 NL/min[4] for >2 h that corresponds to the total amount of supplied hydrogen of >14.4 Nm^3, or >72% of the full hydrogen storage

[4] Up to 170 NL/min during >1 h.

Fig. 8 – MH tank installed in the forklift power module.

capacity of the tank. The H_2 flow rate of 120 NL/min can provide the stack operation at the average power about 11 kWe.[5] The refuelling time of the MH tank at the ambient temperature between 15 and 20 °C is about 15–20 min that is similar to the earlier reported performance of the "distributed hybrid" hydrogen storage system on-board electric forklift with commercial fuel cell power module and MH extension tank which used similar water-cooled MH containers [10]. At the same time, due to the use of a more stable MH material in this work as compared to the material used in Ref. [10], the maximum H_2 dispensing pressure could be lowered from 185 to 100–150 bar.

A brief comparison of features and performances of hydrogen storage tank developed in this work and hydrogen storage tanks for the same electric forklift (RX60-30 L, STILL GmbH) equipped with commercial fuel cell power module (GenDrive 1000 160X-80CEA; Plug Power Inc.) is presented in Table 2. It can be seen that the combination of the CGH2 and MH hydrogen storage implementing the "distributed hybrid" solution [30] significantly lowers the refuelling pressure at a similar hydrogen storage capacity.

Further increase of fraction of H_2 stored in the MH results in the further decrease of the refuelling pressure at the same storage capacity, together with a significant, in ~5 times, decrease of the system volume. Hydrogen storage systems utilising "low-temperature" intermetallic hydrides add weight to the whole on-board power supply system, especially when applying lead encasing procedure described in this work. It is very important for heavy-duty utility vehicle (e.g. forklift) applications where high weight is required for the safe operation.

Due to necessity of dissipation of large amount of heat generated in the MH in the course of system refuelling with H_2, the refuelling time of the MH hydrogen storage systems is longer than for the CGH2 ones. However, the increase of refuelling time for MH systems with optimised thermal management is not very dramatic. Moreover, the slower refuelling allows to significantly reduce overheating of the supplied H_2 thus eliminating necessity of its deep pre-cooling which takes about 10% of the capital costs of the hydrogen refuelling infrastructure [32]. Instead, the refuelling of MH tanks requires their cooling to near-ambient temperatures which can be achieved by simple solutions at the refuelling site and/or in the tank itself.

Since hydrogen desorption from the "low-temperature" MH requires less than 45% of the heat released during the operation of low-temperature fuel cells (e.g. PEMFC) consuming the released H_2 [7], the MH systems can provide H_2 supply to the fuel cell stack which is enough for its operation at the maximum power (see last row of Table2·[6]).

In summary, partial or complete replacement of the CGH2 hydrogen storage system on-board heavy-duty fuel cell utility vehicles (including forklifts) with the MH one brings a number of benefits including decrease of the refuelling pressure thus improving operation safety and lowering costs for the refuelling infrastructure. High weight and compactness of the MH-based hydrogen storage system developed in this work will also allow to reduce the space occupied by a ballast in this kind of vehicles thus adding flexibility to the layout of other components (FC stack + BoP) of the fuel cell power modules which can be further improved towards facilitation of their assembling and service.

The remaining problems planned to be solved at the later stage include (i) further decrease of the refuelling pressure, (ii) the increase of useable (per unit volume) hydrogen storage capacity and (iii) lowering the system cost of which as low as <10% is for the MH material while the remaining costs have to be incurred for the MH containers and other custom-made system components. Solution of the problems (i) and (ii) will be achieved by the optimisation of MH material while the cost reduction (iii) can be achieved by the advancement of

[5] At optimal (towards the increase of stack fuel efficiency) operating conditions. The optimisation of the fuel supply and purging strategy to reduce H_2 consumption and increase the efficiency is in progress.

[6] CGH2 systems are characterized by virtually unlimited rate of the H_2 release. The lower value of maximum H_2 supply flow rate from CGH2 specified in Table 2 is explained by the lower stack power during VDI-60 tests because of reducing, due to safety reasons, the load from the required 3 to 2.5 tonnes [10].

Table 2 – Features and performances of hydrogen storage tanks for fuel cell forklift.

Characteristic		CGH2 tank in the commercial FC power module [31]	CGH2 tank in the commercial FC power module with MH extension tank [10]	MH + CGH2 tank in locally developed FC power module (this work)
Maximum refuelling pressure [bar]		350	185	150
Minimum operating pressure [bar]		13.5	13.5	4
Number of MH containers[a]		–	20	40
Total weight of power module and MH tank installed in the forklift[b]		1600	1784	1830
System inner volume [L]	CGH2	74.2	74.2	9.0
	MH	–	7.4[c]	14.8[c]
	Total	74.2	81.6	23.8
Useable H_2 storage capacity [kg]	CGH2	1.7	0.9	0.1
	MH	–	0.9	1.7
	Total	1.7	1.8	1.8
Refuelling time [min]		3–5	6–15	15–20
Maximum H_2 supply flow rate [NL/min][d]		130	170	170

[a] see Section Metal hydride container
[b] for safe operation of the forklift when lifting the maximum (3 tonne) load, the weight must be between 1800 and 1900 kg
[c] total void volume of the MH containers filled with non-hydrogenated MH material
[d] measured during VDI-60 tests which require the operation of the forklift at the maximum rated power [10].

manufacturing technology of the system components to enable their mass production.

Further details about the design and operation of the developed fuel cell power module with the integrated MH hydrogen storage tank described in this work will be published in a due course.

Conclusions

- New engineering solution of a metal hydride hydrogen storage tank for fuel cell utility vehicles which combines compactness, adjustable high weight, as well as good dynamics of hydrogen charge/discharge has been developed.
- The developed MH tank comprises plurality of MH cassettes made as assemblies of externally heated/cooled MH containers filled with an AB_2-type hydrogen storage material and staggered together with the heating/cooling tubes; the assembly is encased in molten lead followed by the solidification of the latter.
- The MH tank has been successfully integrated in a prototype fuel cell power module for electric forklift.
- Replacement of the CGH2 hydrogen storage system onboard heavy-duty fuel cell utility vehicles with the MH one brings a number of benefits including improvement of operation safety and lowering costs for the refuelling infrastructure.

Acknowledgements

This work is funded by the Department of Science and Technology (DST) within the HySA Programme (HySA Systems projects KP3–S02 and KP6–S03), and Impala Platinum Limited; South Africa. Since end 2017, the international collaboration activities within this work are supported by the EU Horizon 2020 program; Grant Agreement 778307 – HYDRIDE4MOBILITY – H2020-MSCA-RISE-2017.

ML and MWD acknowledge NRF support, grant numbers 109092 (ML) and 116278 (MWD).

The authors also acknowledge engineering and technical support from Hot Platinum (Pty) Ltd (South Africa), in the development and assembling of the forklift fuel cell power module.

REFERENCES

[1] Satyapal S, Petrovic J, Read C, Thomas G, Ordaz G. The U.S. Department of energy's national hydrogen storage project: progress towards meeting hydrogen-powered vehicle requirements. Catal Today 2007;120:246–56.
[2] Godula-Jopek A. Hydrogen storage options including constraints and challenges. In: Godula-Jopek A, editor. Hydrogen production by electrolysis. 1st ed. Wiley-VCH Verlag GmbH & Co. KGaA; 2015. p. 273–309.
[3] Millet P. Hydrogen storage in hydride-forming materials. In: Basile A, Iulianelli A, editors. Advances in hydrogen production, storage and distribution. Elsevier; 2014. p. 368–409. https://doi.org/10.1533/9780857097736.3.368.
[4] Niaz S, Manzoor T, Pandith AH. Hydrogen storage: materials, methods and perspectives. Renew Sustain Energy Rev 2015;50:457–69.
[5] Viswanathan B. Hydrogen storage. In: Energy sources, fundamentals of chemical conversion processes and applications. Elsevier; 2017. p. 185–212. https://doi.org/10.1016/B978-0-444-56353-8.00010-1.
[6] Lototskyy M, Yartys VA. Comparative analysis of the efficiencies of hydrogen storage systems utilising solid state H storage materials. J Alloy Comp 2015;645:S365–73.
[7] Lototskyy MV, Tolj I, Pickering L, Sita C, Barbir F, Yartys V. The use of metal hydrides in fuel cell applications. Prog Nat Sci 2017;27:3–20.

[8] Bellosta von Colbe J, Ares J-R, Barale J, Baricco M, Buckley C, Capurso G, et al. Application of hydrides in hydrogen storage and compression: achievements, outlook and perspectives. Int J Hydrogen Energy 2019;44:7780–808.
[9] Lototskyy MV, Tolj I, Davids MW, Klochko YV, Parsons A, Swanepoel D, et al. Metal hydride hydrogen storage and supply systems for electric forklift with low-temperature proton exchange membrane fuel cell power module. Int J Hydrogen Energy 2016;41:13831–42.
[10] Lototskyy MV, Tolj I, Parsons A, Smith F, Sita C, Linkov V. Performance of electric forklift with low-temperature polymer exchange membrane fuel cell power module and metal hydride hydrogen storage extension tank. J Power Sources 2016;316:239–50.
[11] Jorgensen SW. Hydrogen storage tanks for vehicles: recent progress and current status. Curr Opin Solid State Mater Sci 2011;15:39–43.
[12] Plug power® GenDrive series 1000; http://www.plugpower.com.
[13] HyPX™ POWER PACKS; http://www.hydrogenics.com/.
[14] Technical specifications: H2Drive®. Unlimited and zero emission power for forklifts; http://www.h2logic.com.
[15] Keränen TM, Karimäki H, Viitakangas J, Vallet J, Ihonen J, Hyötylä P, et al. Development of integrated fuel cell hybrid power source for electric forklift. J Power Sources 2011;196:9058–68.
[16] Valicek P, Fourie F. Fuel cell technology in underground mining. In: 6th int. Platinum conf, 'Platinum–Metal for the future'. The Southern African Institute of Mining and Metallurgy; 2014. p. 325–32.
[17] Iwaki T, Itou K, Matsumoto H, Suzuki H, Shibata J, Uematsu N. Hydrogen engine system with metal hydride container. Patent US. 1992. 5 082 048.
[18] Rendina DD. Hydrogen hydride keel. Patent US. 1995. 5 445 099.
[19] Pfeiffer N, Fromme G, Leifert T. Industrial truck with a hydrogen tank. Patent EP. 2005. 1215163 B1.
[20] Gregory BA, Medwin S, Bordwell B, Field M, Banko II JE. Material handling vehicle including integrated hydrogen storage, patent application US. 2009. 0166110 A1.
[21] Narvaez A. Low cost, metal hydride based hydrogen storage system for forklift applications (phase II). US DOE Ann Merit Rev Meeting; June 18, 2014. Project ST 095; https://www.hydrogen.energy.gov/pdfs/review14/st095_narvaez_2014_p.pdf.
[22] Lototskyy M, Davids MW, Pollet BG, Linkov V, Klochko Y. Metal hydride bed, metal hydride container, and method for the making thereof, patent application WO, 2015, 189758 A1.
[23] Lototskyy M, Klochko Y, Tolj I, Davids MW, Parsons A, Sita C, et al. Metal hydride hydrogen storage arrangement for use in a fuel cell utility vehicle and method of manufacturing the same, Patent Application UK 1806840, 3; 2018.
[24] Lototskyy MV, Davids MW, Tolj I, Klochko YV, Satya Sekhar B, Chidziva S, Smith F, Swanepoel D, Pollet BG. Metal hydride systems for hydrogen storage and supply for stationary and automotive low temperature PEM fuel cell power modules. Int J Hydrogen Energy 2015;40:11491–7.
[25] Pickering L, Lototskyy MV, Davids MW, Sita C, Linkov V. Induction melted AB_2-type metal hydrides for hydrogen storage and compression applications. Mater Today: Proc 2018;5:10470–8.
[26] Lototskyy MV. New model of phase equilibria in metal – hydrogen systems: features and software. Int J Hydrogen Energy 2016;41:2739–61.
[27] Rodriguez Sanchez A, Klein H-P, Groll M. Expanded graphite as heat transfer matrix in metal hydride beds. Int J Hydrogen Energy 2003;28:515–27.
[28] Dieterich M, Pohlmann C, Bürger I, Linder M, Röntzsch L. Long-term cycle stability of metal hydride-graphite composites. Int J Hydrogen Energy 2015;40:16375–82.
[29] SANS. (Edition 2), South African National Standard, "Categorization and conformity assessment criteria for all pressure equipment.". 2012.
[30] Lototskyy M, Tolj I, Davids MW, Bujlo P, Smith F, Pollet BG. "Distributed hybrid" MH–CGH2 system for hydrogen storage and its supply to LT PEMFC power modules. J Alloy Comp 2015;645:S329–33.
[31] Service manual: GenDrive series 1000 160x-80CEA, document No: 096136. Plug Power Inc.; 2014.
[32] Elgowainy A, Reddi K, Lee D-Y, Rustagi N, Gupta E. Techno-economic and thermodynamic analysis of pre-cooling systems at gaseous hydrogen refuelling stations. Int J Hydrogen Energy 2017;42:29067–79.